Anion Photoelectron Spectroscopy of C_3N^- and C_5N^-†

Terry A. Yen,‡ Etienne Garand,‡ Alexander T. Shreve,‡ and Daniel M. Neumark*,‡,§

Department of Chemistry, University of California, Berkeley, California 94720, and Chemical Sciences Division, Lawrence Berkeley National Laboratory, Berkeley, California 94720

Received: September 30, 2009; Revised Manuscript Received: November 11, 2009

Anion photoelectron spectroscopy of C_3N^- and C_5N^- is performed using slow electron velocity-map imaging (SEVI) and field-free time-of-flight (TOF), respectively. The SEVI spectrum exhibits well-resolved vibrational transitions from the linear C_3N^- ground state to the corresponding C_3N ground state. The TOF spectrum comprises transitions arising from the linear C_5N^- ground state to the corresponding neutral ground and excited states. This study yields the adiabatic electron affinities of C_3N and C_5N to be 4.305 ± 0.001 and 4.45 ± 0.03 eV, respectively, and a term value of 560 ± 120 cm^{-1} for the $\tilde{A}^2\Pi$ state of C_5N. Vibrational frequencies for the degenerate cis and trans bending modes of C_3N^- are also extracted.

I. Introduction

The recent discoveries of the C_3N and C_5N radicals[1,2] and of the C_3N^- and C_5N^- anions[3,4] in circumstellar envelopes have prompted much interest in characterizing the properties of linear carbon chains of the type $C_{2n+1}N$. In particular, the C_3N radical and C_3N^- anion are key cyanopolyacetylides and important drivers of interstellar chemistry. They are also potentially significant constituents of Titan's ionosphere.[5] The neutral C_3N and C_5N radicals and their anionic counterparts were discovered in the expanding circumstellar envelope of the carbon star IRC + 10216 and in the dark cloud TMC1 with radio telescopes. The interstellar detection of C_3N was confirmed by the observation of the radical in the low-pressure laboratory gas discharge of cyanoacetylene in nitrogen;[6] the corresponding anionic species, C_3N^-, has also been successfully made in the laboratory and has been the subject of a considerable amount of theoretical and experimental effort. Following theoretical predictions by Botschwina,[7] the microwave spectrum of C_5N was measured,[8] yielding its rotational, fine, and hyperfine constants; likewise, the assignment of the B1389 series garnered from the spectral line survey[4] of IRC + 10216 to C_5N^- was significantly aided and confirmed by electronic structure calcuations.[9] The astrophysical relevance of the neutral and anionic species motivates the work described here, in which we report photoelectron spectra of C_3N^- and C_5N^-.

Neutral C_3N is the best characterized of these species. Since Gottlieb et al.[6] found C_3N in the interstellar medium by characterizing the rotational spectrum of the $\tilde{X}^2\Sigma^+$ ground state of C_3N, several infrared and higher-resolution microwave studies have been performed.[3,10–13] Infrared vibrational transitions of C_3N^- produced in rare gas solids via cyanoacetylene dissociation have been reported,[14,15] while high-resolution rotational transitions of C_3N^- produced by discharging a HC_3N:HC_4H gas mixture were observed by McCarthy[12] using Fourier transform microwave spectroscopy. A joint experimental/theoretical study[16] produced millimeter-wave rotational spectra of the ^{13}C isotopic species of C_3N. Endo[11] observed the $\tilde{B}^2\Pi - \tilde{X}^2\Sigma^+$ transition by laser induced fluorescence spectroscopy (LIF) and the $\tilde{A}^2\Pi - \tilde{X}^2\Sigma^+$ transition from dispersed fluorescence (DF). The origin of the $\tilde{A}^2\Pi$ state was determined to lie 1844(3) cm^{-1} above the ground state, and the $\tilde{B}^2\Pi$ state was found to be 27 929.985(2) cm^{-1} above the ground state. Graupner et al.[17] obtained an electron affinity of C_3N of 4.59 ± 0.25 eV by dissociative electron attachment to HC_3N.

There have been several electronic structure calculations predicting the energetics, geometries, infrared vibrational frequencies, and microwave rotational transitions of C_3N and C_3N^-.[14,16,18–21] All predict linear structures for the $\tilde{X}^1\Sigma^+$ ground state of C_3N^- and the $\tilde{X}^2\Sigma^+$ ground state of C_3N. The equilibrium electron affinity of C_3N was recently calculated[14] to be 4.34 eV, ~0.25 eV lower than the experimental value;[17] inclusion of zero-point energies in the calculation increases this discrepancy slightly.

Fewer spectroscopic studies have been reported for C_5N and C_5N^-. The microwave spectrum of C_5N measured by Kasai et al.[8] showed that it was linear with a $\tilde{X}^2\Sigma^+$ ground state. Maier[22] obtained the electronic absorption spectrum of C_5N in a cryogenic matrix by deposition of mass-selected C_5N^- followed by ultraviolet photodetachment, yielding a band around 470 nm that was assigned to the $\tilde{B}^2\Pi \leftarrow \tilde{X}^2\Sigma^+$ transition of C_5N. The IR absorption spectra of C_5N^- generated from vacuum−UV photolysis of cyanodiacetylene (HC_5N) in solid argon have also been identified.[23]

Electronic structure calculations have been reported for C_5N and C_5N^-. Pauzat et al.[24] performed unrestricted Hartree−Fock self-consistent field (UHF-SCF) calculations on the radical that gave an electronic ground state with $^2\Pi$ symmetry. Subsequent coupled cluster (CC) calculations by Botschwina[7,21] disagreed with this result and predicted the electronic ground state of C_5N to have $^2\Sigma^+$ symmetry, with the $^2\Pi$ state lying ~500 cm^{-1} higher in energy. As for the C_5N^- anionic species, Zhan and Iwata[25,26] conducted calculations using Moller−Plesset (MP2) perturbation theory with a 6-31G(d) basis set for anions up to C_7N^- and reported harmonic vibrational frequencies, vertical detachment energies (VDEs), and equilibrium structures. From the optimized geometries of C_nN^- ($n = 4 - 7$) in their ground states, they found that only C_5N^- was linear in its ground state. Later work by Pascoli and Lavendy[27] using density functional theory disagreed with this result and found that all C_nN^- clusters have

† Part of the "Benoît Soep Festschrift".

* Author to whom correspondence should be addressed. E-mail: dneumark@berkeley.edu.

‡ University of California.

§ Lawrence Berkeley National Laboratory.

10.1021/jp9093996
Published on Web 12/10/2009

linear ground state structures. Very recently, Botschwina and Oswald[9] carried out an extensive theoretical study of the $C_{2n+1}N^-$ anions with $n = 2-6$ using CC theory in conjunction with a large basis set that confirmed a linear $^2\Sigma^+$ ground state of the C_5N radical and predicted the equilibrium geometry and the harmonic vibrational frequencies (among other spectroscopic constants) for C_5N^-. The electron affinity of C_5N was calculated to be 4.453 eV.[7]

In this paper, we report anion photoelectron spectra of C_3N^- and C_5N^- obtained with high-resolution slow velocity-map imaging (SEVI) and time-of-flight photoelectron (TOF-PE) spectroscopy. The C_3N^- SEVI spectrum was taken at the photodetachment wavelength of 283 nm (4.382 eV) and shows well-resolved transitions to the neutral $\tilde{X}^2\Sigma^+$ ground state. Franck−Condon (FC) simulations were used to make vibrational assignments within this electronic transition. The TOF-PE spectrum of C_5N^- was taken at 213 nm (5.822 eV) and shows broad transitions assigned to the neutral $\tilde{X}^2\Sigma^+$ ground and $\tilde{A}^2\Pi$ excited states. Experimental adiabatic electron affinities of C_3N and C_5N are determined, along with several anion and neutral vibrational frequencies.

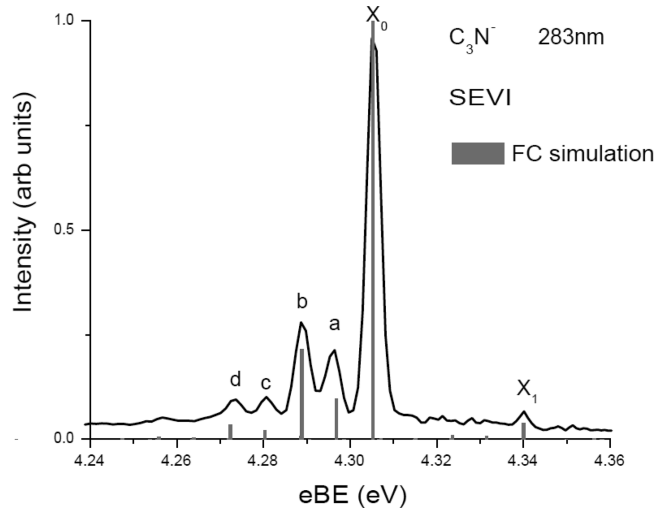

Figure 1. SEVI photoelectron spectrum of C_3N^- at 283 nm (4.382 eV) and plotted in eBE. Overlapped with the spectrum is the Franck−Condon simulation of the peaks in gray.

II. Experimental Section

Photoelectron spectra of C_3N^- and C_5N^- were measured using two spectrometers that employ different electron detection techniques. In our time-of-flight photoelectron (TOF-PE) spectrometer, anions are photodetached using a fixed-frequency laser, and photoelectrons are detected at the end of a field-free time-of-flight (TOF) tube.[28,29] The slow electron velocity-map imaging (SEVI) spectrometer[30–32] yields higher-resolution spectra by photodetaching anions near threshold with a tunable laser and detecting resulting slow photoelectrons using collinear velocity-map imaging.[33] The TOF-PE instrument produces spectra over a wide range of electron kinetic energy with a resolution of 8−10 meV and can operate more easily at higher photon energy, while the SEVI spectrometer yields spectra over a more limited range of electron kinetic energy but with a resolution as high as ∼2 cm^{-1}. C_3N^- was investigated on the SEVI instrument, while the photoelectron spectrum of C_5N^-, with a somewhat higher electron binding energy, was taken on the TOF-PE spectrometer.

In the SEVI spectrometer, C_3N^- anions were produced from a gas mixture of 0.05% acetylene and 2% N_2O in a balance of argon, which was supersonically expanded into the source vacuum chamber through an Even-Lavie pulsed valve.[34] Anions were formed by a discharge source that was described in detail in our previous work on $C_{2n}N^-$ ions.[35] Briefly, the gas mixture was passed through a pair of fine stainless steel meshes separated by 1 mm. An electric discharge was induced by the passage of the gas pulse. This grid discharge source generates cold ions, allowing SEVI to achieve high resolution.

The C_3N^- anions created in the source were injected into a Wiley−McLaren TOF mass spectrometer ($m/\Delta m = 400$)[36] and steered to the interaction region through a series of electrostatic lenses and pinholes. At the interaction region, anions were detached between the extractor and repeller plates of a collinear velocity-map imaging (VMI) stack by a Nd:YAG-pumped tunable dye laser. The resulting photoelectron cloud was then uniformly accelerated and mapped onto a chevron-mounted pair of time-gated, imaging quality microchannel plates (MCPs) coupled to a phosphor screen.[37] Electron hits were recorded using a charge-coupled device (CCD) camera and sent to a computer. Images were collected over 50 000 laser shots, quadrant symmetrized, and inverse-Abel transformed[38] to obtain a 2D slice through the reconstructed 3D photoelectron velocity distribution and then angularly integrated to obtain the photoelectron spectra. The spectra presented here are plotted with respect to electron binding energy (eBE), which is the difference between the incident photon energy and the measured electron kinetic energy. The photoelectron angular distribution (PAD) is given by eq 1 below and was determined directly from the images.

In the TOF-PE spectrometer, C_5N^- anions were generated from cyanoacetylene (synthesized using standard methods[39]) entrained in 10 psi of a <1% acetylene:4.7% NF_3:94.3% Ar gas mixture. The gas was supersonically expanded through a pulsed piezoelectric nozzle followed by a high-voltage discharge at ∼−700−800 V that was stabilized by a 1 keV electron beam. After collimation by a skimmer, anions were injected into a Wiley−McLaren/linear reflection time-of-flight mass spectrometer ($m/\Delta m = 2000$)[40] and photodetached at 213 nm (5.82 eV), the fifth harmonic of a pulsed Nd:YAG laser. A small fraction of these electrons was detected by a pair of chevron-mounted MCPs at the end of a ∼1 m long, magnetically shielded flight tube perpendicular to both the molecular and laser beams. A typical spectrum resulted from collecting 180 000 laser shots.

PADs were obtained by measuring spectra at laser polarization angles $\theta = 0°$ or 90° with respect to the TOF axis. The PAD is given by[41,42]

$$\frac{d\sigma}{d\Omega} = \frac{\sigma_{\text{total}}}{4\pi}\left[1 + \frac{\beta}{2}(3\cos^2\theta - 1)\right] \quad (1)$$

where σ_{total} is the total photodetachment cross section. β is the anisotropy parameter, which varies from −1 to 2 and is given for each feature by

$$\beta = \frac{I_{0°} - I_{90°}}{\frac{1}{2}I_{0°} + I_{90°}} \quad (2)$$

where $I_{0°}$ and $I_{90°}$ are the intensities of the peak taken at laser polarization angles of 0° and 90°, respectively.

III. Results

Figure 1 presents the SEVI spectrum of C_3N^- taken at 283 nm (4.382 eV), plotted in eBE from 4.240 to 4.360 eV. Peak X_0 at 4.305 eV dominates, followed by four small peaks a−d

TABLE 1: Peak Positions in Electronvolts, Anisotropy Parameters, Displacement of Peaks from X_0, and Vibrational and Electronic Assignments for the SEVI Spectrum of C_3N^- Taken at 283 nm[a]

	SEVI			
peak	energy (eV)	β	displacement from X_0 (in cm^{-1})	assignment
d	4.273	0.6 ± 0.1	−258	4_2^2 $\tilde{X}^2\Sigma^+ \leftarrow \tilde{X}^1\Sigma^+$
c	4.281	0.6 ± 0.1	−194	$4_1^1 5_1^1$
b	4.289	0.6 ± 0.1	−129	4_1^1
a	4.296	0.6 ± 0.1	−73	5_1^1
X_0	4.305	0.5 ± 0.1	0	0_0^0
X_1	4.339	0.5 ± 0.1	274	5_0^2

[a] Vibrational modes: $\nu_1(\sigma)$ pseudosym stretch, ν_2 (σ) pseudoasym stretch, $\nu_3(\sigma)$ middle C−C stretch, $\nu_4(\pi)$ cis bend, $\nu_5(\pi)$ trans bend.

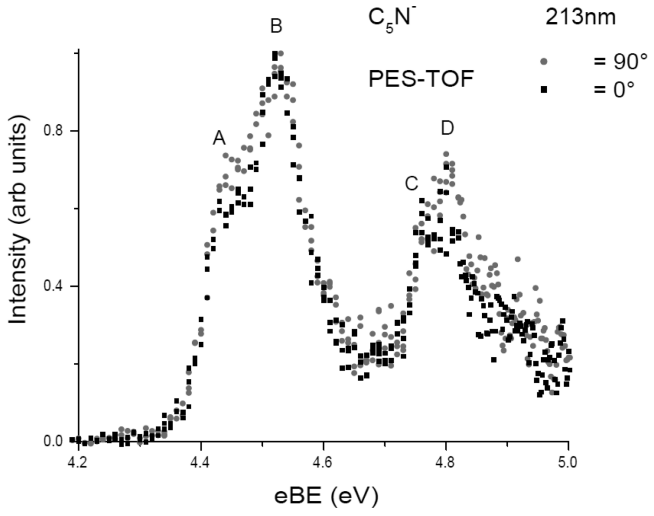

Figure 2. TOF-PE spectra of C_5N^- at 213 nm (5.822 eV) plotted in eBE. The traces are taken at laser polarization angles of 0° and 90°.

at slightly lower eBE and one smaller peak, X_1, lying at 35 meV higher eBE than X_0. All peaks have anisotropy parameters of 0.5−0.6, as seen in Table 1.

TOF-PE spectra of C_5N^- taken at 213 nm are shown in Figure 2, with the spectrum at a laser polarization angle of 0° (in gray) overlaid on the spectrum at 90° (in black). The spectra are plotted in eBE between 4.20 and 5.00 eV, and intensities are scaled relative to the raw TOF data. No features were seen below 4.30 eV; at higher eBE, four fairly broad peaks, A, B, C, and D, are seen. Table 2 lists the anisotropy parameters of these peaks. Feature A is slightly more intense at $\theta = 0°$ with $\beta = 0.2$, while peaks B, C, and D are isotropic ($\beta = 0$) with intensities that are insensitive to the laser polarization angle.

IV. Discussion

A. Vibrational Assignments of the SEVI Spectrum of C_3N^-. In Figure 1, peak X_0 is clearly the vibrational origin, and the dominance of this feature indicates that there is relatively little geometry change upon photodetachment of C_3N^-. The smaller peaks can be assigned with reference to the previously calculated results for the anion and neutral summarized in Table 3. Peaks a−d, which occur at lower eBE than X_0, must arise from vibrationally excited anion levels, most likely the low-frequency ν_4 and ν_5 bending modes. In the photoelectron spectrum, only even $\Delta\nu$ transitions are allowed for these two nontotally symmetric modes, suggesting that these peaks are sequence band ($\Delta\nu = 0$) transitions from bend-excited states whose displacement from the origin reflects differences in the anion and neutral vibrational frequencies.

To confirm this assignment, Franck−Condon (FC) simulations of the degenerate bending modes were employed. These simulations were carried out treating each mode as an independent harmonic oscillator and using the parallel mode approximation, which neglects Duschinsky rotation[43] between the modes. The vibrational temperature and the known calculated and experimental anion and neutral vibrational frequencies were used as inputs into the PESCAL program by Ervin and co-workers.[44–46] This program uses the recursion relation method of Hutchisson[47] to calculate the FC factors and output a simulated photoelectron spectrum.

Figure 1 compares the SEVI spectrum with the stick FC simulation of the $\tilde{X}^2\Sigma^+ \leftarrow \tilde{X}^1\Sigma^+$ transition. The origin of the simulation was chosen to match X_0, the expected vibrational origin of the spectrum. Table 1 gives peak assignments from the simulation. As inputs for the simulation, we used vibrational temperatures of 350 K for ν_4 and 100 K for ν_5, experimental values[11] for the ν_4 and ν_5 fundamental transitions in the ground state of the neutral C_3N, and, initially, calculated values[14] for ν_4 and ν_5 of the ground state of C_3N^- that were modified to produce a better fit. The optimized values for the ν_4 and ν_5 bending modes in C_3N^- obtained from this procedure are 538 ± 8 and 208 ± 8 cm^{-1}, as listed in Table 3. These values agree with the RCCSD(T) calculations.[14]

The simulated spectrum matches our spectrum quite well with all the major peaks reproduced. Peaks d, c, b, and a are assigned to the $\Delta\nu = 0$ sequence of ν_4 and ν_5, with peak a being the 5_1^1 transition, peak b the 4_1^1 band, peak c the $4_1^1 5_1^1$ combination band, and peak d the 4_2^2 transition. Peak X_1, 274 cm^{-1} above the origin, is assigned to the 5_0^2 transition; this displacement agrees with that observed previously via dispersed fluorescence from the $\tilde{B}$ state of C_3N[11], within the error bars of our experiment. From the eBE of the band origin, peak X_0, we obtain the electron affinity (EA) of C_3N, 4.305 ± 0.001 eV. As seen in Table 4, this value is close to but lower than the calculated equilibrium EA of 4.344 eV.[14]

B. Band Assignments of TOF-PE Spectrum of C_5N^-. The TOF-PE spectrum of C_5N^- can be tentatively assigned with reference to the experimental and calculated geometries and frequencies summarized in Table 5 and energetics in Table 6. Peaks A and B are separated by ~560 cm^{-1} and do not appear to be the start of a vibrational progression as there are only two peaks. However, the spacing is very close to the calculated energy splitting between the neutral $\tilde{X}^2\Sigma^+$ ground and $\tilde{A}^2\Pi$ excited states[7] of 500 cm^{-1} (Table 6). In addition, peaks A and B have slightly different PADs (Table 2). Hence, we attribute peaks A and B to the vibrational origins of the neutral $\tilde{X}^2\Sigma^+$ and $\tilde{A}^2\Pi$ states, respectively. This assignment of peak A gives EA (C_5N) $= 4.45 \pm 0.03$ eV, which is in close agreement with the calculated value of 4.453 eV (see Table 6).[7]

Peaks C and D then appear to be transitions to vibrationally excited levels of one or both of these states. To try to assign these features, and since no experimental or vibrational frequen-

TABLE 2: Peak Positions in Electronvolts, Angular Distributions (PAD), Displacement of Peaks from A, and Vibrational and Electronic Assignments for the TOF-PE Spectrum of C_5N^- Taken at 213 nm[a]

	TOF-PE			
peak	energy (eV)	β	displacement from A (in cm^{-1})	tentative assignment
A	4.45	0.2 ± 0.1	0	0_0^0 $\tilde{X}^2\Sigma^+ \leftarrow \tilde{X}^1\Sigma^+$
B	4.52	0 ± 0.1	565	0_0^0 $\tilde{X}^2\Sigma^+ \leftarrow \tilde{A}^2\Pi$
C	4.76	0 ± 0.1	2500	3_0^1 $\tilde{X}^2\Sigma^+ \leftarrow \tilde{A}^2\Pi$
D	4.80	0 ± 0.1	2823	1_0^1 $\tilde{X}^2\Sigma^+ \leftarrow \tilde{A}^2\Pi$

[a] Vibrational modes: $\nu_1(\sigma)$, $\nu_2(\sigma)$, $\nu_3(\sigma)$, $\nu_4(\sigma)$, and $\nu_5(\sigma)$ are the various active stretching modes, while $\nu_6(\pi)$, $\nu_7(\pi)$, $\nu_8(\pi)$, and $\nu_9(\pi)$ are the active bending modes.

TABLE 3: Calculated Geometries and Vibrational Frequencies of the C_3N^- Anion and C_3N Radical from Current and Previous Calculations and Experiment[a]

C_3N species		$r(C_1C_2)$	$r(C_2C_3)$	$r(C_3N)$	$\nu_1(\sigma)$	$\nu_2(\sigma)$	$\nu_3(\sigma)$	$\nu_4(\pi)$	$\nu_5(\pi)$
$^1\Sigma^+$ (anion)	CCSD(T)/aug-cc-pCV5Z (empirically corr.)[c]	1.252	1.366	1.171					
	CCSD(T)/aug-cc-pVQZ[c]				2210	1965	876	533	203
	expt. SEVI[d]	-	-	-	-	-	-	538 ± 8	208 ± 8
$^2\Sigma^+$ (neutral)	CASSCF[e]	1.217	1.388	1.160	-	-	-	-	-
	CEPA-1 (112cGTOs)[f]	1.214	1.385	1.162	2280 ± 15	2090 ± 15	883 ± 15	-	-
	RCCSD(T)/rec.[g,b]	1.210	1.377	1.160	-	-	-	-	-
	RCCSD(T)/val[h]	-	-	-	2312	2117	885	414	147
	RCCSD/all+(T)/val/cc-pVQZ[h]	1.210	1.377	1.160	-	-	-	-	-
	RCCSD(T)/val/cc-pVTZ + expt.[h]	1.212	1.375	1.161	-	-	-	-	-
	expt. LIF[i]	-	-	-	-	-	1054	405	131

[a] Vibrational modes: $\nu_1(\sigma)$ pseudosym stretch, $\nu_2(\sigma)$ pseudoasym stretch, $\nu_3(\sigma)$ middle C−C stretch, $\nu_4(\pi)$ cis bend, $\nu_5(\pi)$ trans bend. All frequencies except for the CEPA-1 (112cGTOs) of the $^2\Sigma^+$ state are harmonic frequencies. [b] Recommended equilibrium structures based on calculations involving RCCSD(T). [c] Ref 14. [d] This work. [e] Ref 19. [f] Ref 18. [g] Ref 23. [h] Ref 16. [i] Ref 11.

TABLE 4: Calculated and Experimental Transition Energies between Selected States of the C_3N Anion and Neutral[a]

transition	ΔE (eV)	method
$\tilde{X}^1\Sigma^+ \rightarrow \tilde{X}^2\Sigma^+$ *	4.344**	RCCSD(T)/aug-cc-pV5Z[b]
	4.59 ± 0.25	expt. dissociative attachment[g]
	4.305 ± 0.001	expt. SEVI[c]
$\tilde{X}^2\Sigma^+ \rightarrow \tilde{A}^2\Pi$	0.229 (1844 cm^{-1})	expt. LIF[d]
	0.267 (2150 ± 150 cm^{-1})	RCCSD(T)/cc-pVTZ[e]
	0.186 (1500 ± 50 cm^{-1})	CASSCF (148cGTOs)[f]
$\tilde{A}^2\Pi \rightarrow \tilde{B}^2\Pi$	3.463 (27929.985 cm^{-1})	expt. LIF[d]

[a] Transitions marked with an asterisk can be observed in the photoelectron spectra; the remaining ones are neutral−neutral transitions. Numbers marked with a double asterisk are equilibrium energies; the unmarked ones are adiabatic energies. [b] Ref 14. [c] This work. [d] Ref 11. [e] Ref 16. [f] Ref 18. [g] Ref 17.

TABLE 5: Calculated Geometries and Vibrational Frequencies of the C_5N^- Anion and C_5N Radical from Current and Previous Calculations and Experiment[a]

C_5N species		$r(C_1C_2)$	$r(C_2C_3)$	$r(C_3C_4)$	$r(C_4C_5)$	$r(C_5N)$	$\nu_1(\sigma)$	$\nu_2(\sigma)$	$\nu_3(\sigma)$	$\nu_4(\sigma)$	$\nu_5(\sigma)$	$\nu_6(\pi)$	$\nu_7(\pi)$	$\nu_8(\pi)$	$\nu_9(\pi)$
$^1\Sigma^+$ (anion)	CCSD(T)/vqz+[b,d]	1.258	1.345	1.231	1.357	1.170	2236	2156	1951	1179	620	503	494	227	97
	expt. Far-UV irradiation of cyanodiacetylene (HC_5N) in solid argon[g]	-	-	-	-	-	2184	2111	1923	-	-	-	-	-	-
	B3LYP/aug-cc-pVTZ[e]	1.253	1.337	1.230	1.349	1.168	2275	2204	2001	1214	638	551	521	253	107
$^2\Sigma^+$ (neutral)	RCCSD(T)/180 cGTOs[f]	1.214*	1.366*	1.212*	1.371*	1.161*	2319	2226	2098	1163	612	-	-	-	-
	RCCSD(T)/rec.[h,c]	1.214	1.365	1.212	1.371	1.162	-	-	-	-	-	-	-	-	-
	B3LYP/aug-cc-pVTZ[e]	1.209	1.355	1.211	1.361	1.157	2342	2275	2158	1206	634	1254	543	332	121
$^2\pi$ (neutral)	RCCSD(T)/180 cGTOs[f]	1.296*	1.328*	1.229*	1.362*	1.164*	-	-	-	-	-	-	-	-	-
	RCCSD(T)/rec.[h,c]	1.296	1.328	1.230	1.362	1.164	-	-	-	-	-	-	-	-	-
	B3LYP/aug-cc-pVTZ[e]	1.286	1.313	1.236	1.345	1.163	2215	2108	1906	1205	638	-	-	-	-

[a] Vibrational modes: $\nu_1(\sigma)$, $\nu_2(\sigma)$, $\nu_3(\sigma)$, $\nu_4(\sigma)$, and $\nu_5(\sigma)$ are the various active stretching modes, while $\nu_6(\pi)$, $\nu_7(\pi)$, $\nu_8(\pi)$, and $\nu_9(\pi)$ are the active bending modes for the linear molecules. All frequencies calculated are harmonic frequencies. Bond lengths marked with an asterisk are empirically corrected values. [b] cc-pVQZ at all atoms plus the diffuse s, p, d, f, and g functions from the aug-cc-pVQZ for the terminal atoms. [c] Recommended equilibrium structures based on calculations involving RCCSD(T). [d] Ref 9. [e] This work. [f] Ref 7. [g] Ref 23. [h] Ref 21.

cies were available for the $\tilde{A}^2\Pi$ state, electronic structure calculations were performed on neutral and anionic C_5N. Density functional calculations were performed using the Becke three-parameter Lee−Yang−Parr exchange-correlation functional[48,49] (B3LYP) with the augmented correlation consistent polarized valence triple-ζ set[50] (aug-cc-pVTZ). All calculations were

TABLE 6: Calculated and Experimental Transition Energies between Selected States of the C_5N Anion and Neutral[a]

transition	ΔE	method
$\tilde{X}^1\Sigma^+ \rightarrow \tilde{X}^2\Sigma^+$ *	4.453 eV	RCCSD(T)/234 cGTOs
	4.45 ± 0.03 eV	expt. TOF-PE[c]
$\tilde{X}^2\Sigma^+ \rightarrow \tilde{A}^2\Pi$	500 cm^{-1}**	CCSD(T)/cc-pVTZ[b]
	560 ± 120 cm^{-1}	expt. TOF-PE[c]

[a] Transitions marked with an asterisk can be observed in the photoelectron spectra; the remaining ones are neutral−neutral transitions. Numbers marked with a double asterisk are equilibrium energies; the unmarked ones are adiabatic energies. [b] Ref 7. [c] This work.

carried out using the GAUSSIAN03 program.[51] Table 5 compares our calculations to previous values; we report only the frequencies of the stretching modes of the $\tilde{A}^2\Pi$ state.

For the C_5N^- $\tilde{X}^1\Sigma^+$ state, our optimized geometry and calculated vibrational frequencies match up reasonably well with the values reported by Botschwina and Oswald[9] that were obtained using CCSD(T)/cc-pVQZ for all atoms plus the aug-cc-pVQZ for the terminal atoms. Our B3LYP frequencies are within 50 cm^{-1} and our bond lengths within 0.008 Å. Detachment from the nonbonding σ orbital on the terminal carbon leads to the neutral $\tilde{X}^2\Sigma^+$ state. Our optimized geometry and calculated harmonic vibrational frequencies for the stretching modes of this state C_5N match up with the RCCSD(T) calculations of Botschwina.[7] Our B3LYP frequencies for the five stretches of C_5N are within 50 cm^{-1}, and our bond lengths within 0.01 Å. Detachment from a π orbital leads to the $\tilde{A}^2\Pi$ state of the neutral species which was also calculated to be linear.[7] Our optimized bond lengths for this state are within 0.02 Å of that work.

The spacing between peaks A and C is 0.31 ± 0.03 eV (2500 cm^{-1}), which is larger than any fundamental frequencies of the neutral $\tilde{X}^2\Sigma^+$ state. However, our calculated frequency of 1906 cm^{-1} for the ν_3 stretching mode of the neutral $\tilde{A}^2\Pi$ state is close to the spacing of 0.24 ± 0.03 eV (1940 cm^{-1}) between peaks B and C. Peak D is 0.28 ± 0.03 eV (2260 cm^{-1}) higher in eBE than peak B, close to our calculated frequency of 2215 cm^{-1} for the ν_1 stretching mode. Moreover, Table 2 shows that B, C, and D have roughly the same PADs. We thus tentatively assign peaks B, C, and D as the vibrational origin, 3_0^1, and 1_0^1 photodetachment transitions to the $\tilde{A}^2\Pi$ state.

The peaks in the TOF-PE spectrum of C_5N^- are surprisingly broad, considering that the anion and neutral are expected to be linear.[7,9,22] The peak widths may reflect a high anion vibrational temperature, resulting in spectral congestion from $\Delta v = 0$ sequence bands originating from vibrationally excited bending levels of the anion, several of which have quite low frequencies (Table 5, first row). The resulting sequence bands would not be resolved in the TOF-PE spectra, in contrast to the higher resolution SEVI spectrum of C_3N^-. In addition, the closely spaced $\tilde{X}^2\Sigma^+$ and $\tilde{A}^2\Pi$ states of C_5N will be vibronically coupled via the bending modes, all of which have π symmetry, resulting in activation of normally forbidden $\Delta v = 1$ transitions in these modes for photodetachment to both neutral states.[52] Such transitions, again involving low-frequency modes, will result in further spectral congestion.

V. Conclusions

Photoelectron spectra of C_3N^- and C_5N^- were obtained using slow electron velocity-map imaging (SEVI) and TOF photoelectron (TOF-PE) spectroscopy, respectively. From the SEVI spectrum, vibrational transitions to the ground $\tilde{X}^2\Sigma^+$ state of neutral C_3N were resolved, allowing accurate experimental determinations of the electron affinity of C_3N, 4.305 ± 0.001 eV, as well as frequencies of the degenerate bending modes of C_3N^-. The lesser quality C_5N^- TOF-PE spectra allowed only a tentative assignment of the observed features to the ground $\tilde{X}^2\Sigma^+$ and low-lying $\tilde{A}^2\Pi$ states, as well as to vibrational features of the $\tilde{A}^2\Pi$ state. This assignment yields an electron affinity of 4.45 ± 0.03 eV for C_5N and a term value of 560 ± 120 cm^{-1} for the $\tilde{A}^2\Pi$ state.

Acknowledgment. This work was supported by the National Science Foundation under Grant No. CHE-0649647. E.G. thanks the National Science and Engineering Research Council of Canada (NSERC) for a postgraduate scholarship.

References and Notes

(1) Guelin, M.; Thaddeus, P. *Astrophys. J.* **1977**, *212*, L81.
(2) Guelin, M.; Neininger, N.; Cernicharo, J. *Astron. Astrophys.* **1998**, *335*, L1.
(3) Thaddeus, P.; Gottlieb, C. A.; Gupta, H.; Brunken, S.; McCarthy, M. C.; Agundez, M.; Guelin, M.; Cernicharo, J. *Astrophys. J.* **2008**, *677*, 1132.
(4) Cernicharo, J.; Guelin, M.; Agundez, M.; McCarthy, M. C.; Thaddeus, P. *Astrophys. J.* **2008**, *688*, L83.
(5) Coates, A. J.; Crary, F. J.; Lewis, G. R.; Young, D. T.; Waite, J. H.; Sittler, E. C. *Geophys. Res. Lett.* **2007**, *34*, 6.
(6) Gottlieb, C. A.; Gottlieb, E. W.; Thaddeus, P.; Kawamura, H. *Astrophys. J.* **1983**, *275*, 916.
(7) Botschwina, P. *Chem. Phys. Lett.* **1996**, *259*, 627.
(8) Kasai, Y.; Sumiyoshi, Y.; Endo, Y.; Kawaguchi, K. *Astrophys. J.* **1997**, *477*, L65.
(9) Botschwina, P.; Oswald, R. *J. Chem. Phys.* **2008**, *129*, 11.
(10) Guennoun, Z.; Couturier-Tamburelli, I.; Pietri, N.; Aycard, J. P. *Chem. Phys. Lett.* **2003**, *368*, 574.
(11) Hoshina, K.; Endo, Y. *J. Chem. Phys.* **2007**, *127*, 12.
(12) McCarthy, M. C.; Thaddeus, P. *J. Chem. Phys.* **2008**, *129*, 6.
(13) Crepin, C.; Moneron, L.; Douin, S.; Boye-Peronne, S.; Kolos, R.; Turowski, M.; Gronowski, M.; Sepiol, J.; Benilan, Y.; Gazeau, M. C. *Pol. J. Chem.* **2008**, *82*, 741.
(14) Kolos, R.; Gronowski, M.; Botschwina, P. *J. Chem. Phys.* **2008**, *128*, 11.
(15) Khriachtchev, L.; Lignell, A.; Tanskanen, H.; Lundell, J.; Kiljunen, H.; Rasanen, M. *J. Phys. Chem. A* **2006**, *110*, 11876.
(16) McCarthy, M. C.; Gottlieb, C. A.; Thaddeus, P.; Horn, M.; Botschwina, P. *J. Chem. Phys.* **1995**, *103*, 7820.
(17) Graupner, K.; Merrigan, T. L.; Field, T. A.; Youngs, T. G. A.; Marr, P. C. *New J. Phys.* **2006**, *8*, 17.
(18) Botschwina, P.; Horn, M.; Flugge, J.; Seeger, S. *J. Chem. Soc., Faraday Trans.* **1993**, *89*, 2219.
(19) Sadlej, J.; Roos, B. O. *Chem. Phys. Lett.* **1991**, *180*, 81.
(20) Francisco, J. S. *Chem. Phys. Lett.* **2000**, *324*, 307.
(21) Botschwina, P. *Phys. Chem. Chem. Phys.* **2003**, *5*, 3337.
(22) Grutter, M.; Wyss, M.; Maier, J. P. *J. Chem. Phys.* **1999**, *110*, 1492.
(23) Coupeaud, A.; Turowski, M.; Gronowski, M.; Pietri, N.; Couturier-Tamburelli, I.; Kolos, R.; Aycard, J. P. *J. Chem. Phys.* **2008**, 128.
(24) Pauzat, F.; Ellinger, Y.; McLean, A. D. *Astrophys. J.* **1991**, *369*, L13.
(25) Zhan, C. G.; Iwata, S. *J. Chem. Phys.* **1996**, *104*, 9058.
(26) Zhan, C. G.; Iwata, S. *J. Chem. Phys.* **1996**, *105*, 6578.
(27) Pascoli, G.; Lavendy, H. *Chem. Phys. Lett.* **1999**, *312*, 333.
(28) Xu, C. S.; Burton, G. R.; Taylor, T. R.; Neumark, D. M. *J. Chem. Phys.* **1997**, *107*, 3428.
(29) Metz, R. B.; Weaver, A.; Bradforth, S. E.; Kitsopoulos, T. N.; Neumark, D. M. *J. Phys. Chem.* **1990**, *94*, 1377.
(30) Osterwalder, A.; Nee, M. J.; Zhou, J.; Neumark, D. M. *J. Chem. Phys.* **2004**, *121*, 6317.
(31) Zhou, J.; Garand, E.; Neumark, D. M. *J. Chem. Phys.* **2007**, *127*, 9.
(32) Neumark, D. M. *J. Phys. Chem. A* **2008**, *112*, 13287.
(33) Eppink, A.; Parker, D. H. *Rev. Sci. Instrum.* **1997**, *68*, 3477.
(34) Even, U.; Jortner, J.; Noy, D.; Lavie, N.; Cossart-Magos, C. *J. Chem. Phys.* **2000**, *112*, 8068.
(35) Garand, E.; Yacovitch, T. I.; Neumark, D. M. *J. Chem. Phys.* **2009**, *130*, 7.
(36) Wiley, W. C.; McLaren, I. H. *Rev. Sci. Instrum.* **1955**, *26*, 1150.
(37) Chandler, D. W.; Houston, P. L. *J. Chem. Phys.* **1987**, *87*, 1445.
(38) Hansen, E. W.; Law, P. L. *J. Opt. Soc. Am. A-Opt. Image Sci. Vis.* **1985**, *2*, 510.

(39) Miller, F. A.; Lemmon, D. H. *Spectrochim. Acta A-Mol. Spectrosc.* **1967**, *A 23*, 1415.
(40) Markovich, G.; Giniger, R.; Levin, M.; Cheshnovsky, O. *J. Chem. Phys.* **1991**, *95*, 9416.
(41) Cooper, J.; Zare, R. N. *J. Chem. Phys.* **1968**, *48*, 942.
(42) Reid, K. L. *Annu. Rev. Phys. Chem.* **2003**, *54*, 397.
(43) Duschinsky, F. *Acta Physicochim. URSS* **1937**, *7*, 551.
(44) Ervin, K. M.; Ho, J.; Lineberger, W. C. *J. Chem. Phys.* **1989**, *91*, 5974.
(45) Ervin, K. M.; Ramond, T. M.; Davico, G. E.; Schwartz, R. L.; Casey, S. M.; Lineberger, W. C. *J. Phys. Chem. A* **2001**, *105*, 10822.
(46) Ervin, K. M. PESCAL (FORTRAN), 2001.
(47) Hutchisson, E. *Phys. Rev.* **1930**, *36*, 0410.
(48) Becke, A. D. *J. Chem. Phys.* **1993**, *98*, 1372.
(49) Lee, C. T.; Yang, W. T.; Parr, R. G. *Phys. Rev. B* **1988**, *37*, 785.
(50) Dunning, T. H. *J. Chem. Phys.* **1989**, *90*, 1007.
(51) Frisch, M. J.; Trucks, G. W.; Schlegel, H. B.; Scuseria, G. E.; Robb, M. A.; Cheeseman, J. R.; Montgomery, J. A., Jr.; Vreven, T.; Kudin, K. N.; Burant, J. C.; Millam, J. M.; Iyengar, S. S.; Tomasi, J.; Barone, V.; Mennucci, B.; Cossi, M.; Scalmani, G.; Rega, N.; Petersson, G. A.; Nakatsuji, H.; Hada, M.; Ehara, M.; Toyota, K.; Fukuda, R.; Hasegawa, J.; Ishida, M.; Nakajima, T.; Honda, Y.; Kitao, O.; Nakai, H.; Klene, M.; Li, X.; Knox, J. E.; Hratchian, H. P.; Cross, J. B.; Bakken, V.; Adamo, C.; Jaramillo, J.; Gomperts, R.; Stratmann, R. E.; Yazyev, O.; Austin, A. J.; Cammi, R.; Pomelli, C.; Ochterski, J. W.; Ayala, P. Y.; Morokuma, K.; Voth, G. A.; Salvador, P.; Dannenberg, J. J.; Zakrzewski, V. G.; Dapprich, S.; Daniels, A. D.; Strain, M. C.; Farkas, O.; Malick, D. K.; Rabuck, A. D.; Raghavachari, K.; Foresman, J. B.; Ortiz, J. V.; Cui, Q.; Baboul, A. G.; Clifford, S.; Cioslowski, J.; Stefanov, B. B.; Liu, G.; Liashenko, A.; Piskorz, P.; Komaromi, I.; Martin, R. L.; Fox, D. J.; Keith, T.; Al-Laham, M. A.; Peng, C. Y.; Nanayakkara, A.; Challacombe, M.; Gill, P. M. W.; Johnson, B.; Chen, W.; Wong, M. W.; Gonzalez, C.; Pople, J. A. *Gaussian 03*, revision C.02; Gaussian, Inc.: Wallingford, CT, 2004.
(52) Zhou, J.; Garand, E.; Neumark, D. M. *J. Chem. Phys.* **2007**, *127*, 154320.

JP9093996